3D-QSAR studies on antitubercular thymidine monophosphate kinase inhibitors based on different alignment methods

V. Aparna,[a] J. Jeevan,[a] M. Ravi,[a] G. R. Desiraju[a,*] and B. Gopalakrishnan[b,*]

[a]*School of Chemistry, University of Hyderabad, Hyderabad 500 046, India*
[b]*Life Sciences R&D Division, Advanced Technology Centre, TATA Consultancy Services Limited,*
1 Software Units Layout, Madhapur, Hyderabad 500 081, India

Abstract—Three dimensional quantitative structure–activity relationship (3D-QSAR) studies were carried out on deoxythymidine monophosphate (dTMP) derivatives inhibiting thymidine monophosphate kinase (TMPK) in *Mycobacterium tuberculosis*. Molecular field analysis (MFA) models with three different alignment techniques, namely, least squares, pharmacophore based and receptor based methods were developed. Receptor based MFA model showed better results when compared with least squares and pharmacophore based models. The results help us to understand the nature of substituents required for activity and thereby provide guidelines to design novel and potent inhibitors as antitubercular agents.
© 2005 Elsevier Ltd. All rights reserved.

Tuberculosis (TB) is alarmingly on the rise.[1] Approximately, one third of the world's population is infected with TB bacillus, *Mycobacterium tuberculosis*, with more than 8 million people contracting the disease and 2 million people dying of it each year.[2] A peculiar aspect of its pathogenicity comes from the fact that it can remain quiescent and become active decades later. One of the most significant risk factors for developing tuberculosis is human immunodeficiency virus (HIV) infection.[3] The World Health Organisation (WHO) reports that in Africa 80% of the cases with TB are HIV infected. The current treatment of active TB includes a dosage regime of four drugs (isoniazid, rifampicin, pyrazinamide, and ethambutol) for at least six months. As a consequence of the prolonged duration, irregular treatment, and the highly adaptive nature of the organisms to their surroundings, multidrug resistant (MDR) strains of *M. tuberculosis* have developed. Therefore, the urgent need to cope with the current crisis has stimulated the search for

new targets and the development of new antibiotic drugs to meet the global emergency.

M. tuberculosis thymidine monophosphate kinase (TMPK$_{mt}$) belongs to a large super family of nucleoside monophosphate kinases (NMPK). It catalyses the phosphorylation of deoxythymidine monophosphate (dTMP) to deoxythymidine diphosphate (dTDP) utilizing ATP as a phosphoryl donor. This step lies at the junction of the de novo and salvage pathways of thymidine triphosphate (TTP) metabolism and is the last specific enzyme for its synthesis.[4] Also, the sequence of TMPK$_{mt}$ when compared with that of its human isozyme shows only 22% sequence identity.[5] These characteristics make TMPK$_{mt}$ one of the potential targets for the design of new antitubercular drugs.

Several dTMP derivatives were synthesized and studied for their effect on the TMPK$_{mt}$.[6–9] Structure–activity relationship studies on these reveal that a halogen substitution at position-5 reflects the size effect, with the halogen serving as a cavity filler.[10] In the present study, 3D-QSAR analyses were carried out on a series of dTMP analogues, to gain further insight into the key structural features required to design potential drug candidates of this class. The fact that the reliability and

the efficiency of 3D-QSAR methods depend on the orientation of the molecule[11] prompted us to generate and compare molecular field analysis (MFA) models using different alignment methods.

Selection of molecules. A data set of 47 compounds reported as thymidine monophosphate kinase inhibitors was collected from the literature (Table 1).[6–9] The inhibitory activities were converted into the corresponding pK_i ($-\log K_i$) values, where the K_i value represents the drug concentration that causes inhibition of dTMP phosphorylation by $TMPK_{mt}$. All the K_i values had been obtained by the same assay method.[7] pK_i values of all the molecules spanned a sufficiently wide range from 2 to 6. The training/test set selection was done manually such that they populate the wide range of activities in similar proportions.

All the molecules were built from the coordinates of dTMP structure (1G3U) using the builder module of Cerius^2.[12] All the structures were minimized using the steepest descent algorithm with a convergence gradient value of 0.001 kcal/mol. Partial atomic charges were calculated using the Gasteiger method. Further geometry optimization was carried out for each compound with the MOPAC 6 package using the semi-empirical AM1 Hamiltonian.

Three different alignment methods that were used for MFA are detailed as follows.

Model I (least squares alignment): This alignment was carried out using the shape reference method in the QSAR module within Cerius^2 using the six thymidine ring atoms. The most active compound **38** was used as a template for superposing the rest of the molecules. The aligned molecules are shown in Figure 1a. From the 47 compounds above, 35 were used in the training set and the remaining 12 compounds were included in the test set.

Model II (pharmacophore based alignment): A pharmacophore model was developed using the CATALYST[13] HypoGen module (published elsewhere).[14] The studied molecules were superimposed on the best pharmacophore model using the 'best fit' method. The conformation of each molecule is selected based on the lowest rmsd between the pharmacophoric features and the corresponding functional groups present in the molecule. Figure 1b shows the alignment obtained. Out of the 47 molecules, 35 molecules were used as training set and the remaining 12 molecules were selected as test set.
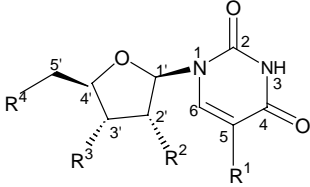
Model III (receptor based alignment): Docking was carried out using the program GOLD.[15] The details of the docking setup are illustrated in Ref. 14. The docking run produces ten conformations for each molecule. Out of these, the best docking conformation for each molecule is selected based on GOLD score. Figure 1c shows the overlay diagram of the ligand conformations within the binding pocket of the $TMPK_{mt}$. Thirtyfour of fortyseven molecules were selected as the training set leaving the other 13 molecules as test set.

MFA. Alternate probes like NH_2 and H_2O were used to calculate the electrostatic interaction energy. The geometry of H_2O probe was optimized at the 6-31G* level using Gaussian 03 and the corresponding charges were used for the calculation of interaction energies. In the case of the NH_2 probe, an arginine molecule was taken as template and optimized at the 6-31G* level. The charges corresponding to the side chain guanidinium NH_2 of arginine were considered, while adjusting the total charge of the probe to +0.1.

MFA studies were performed with the QSAR module of Cerius^2. The molecular field was created using CH_3, NH_2 and H_2O as probes representing steric and electrostatic fields, respectively. The steric and electrostatic fields were sampled at each point of a regularly spaced grid of 1 Å. A number of spatial and structural descriptors such as polarizability, dipole moment, radius of gyration, number of rotatable bonds, molecular volume, principle moments of inertia, $A \log P$, number of hydrogen bond donors and acceptors, and molar refractivity were considered along with the steric and electrostatic descriptors. Only 10% of the total descriptors whose variance was highest were considered for further analysis. Regression analysis was carried out using genetic partial least squares (G/PLS) method consisting of over 50,000 generations with a population size of 100. The optimal number of components was set to eight based on better r^2 and r_{cv}^2 values for a given training set. An energy cutoff of ±30.0 kcal/mol was set for both steric and electrostatic contributions. The smoothing parameter, d, was set to 1.0 to control the bias in the scoring factors between equations with different number of terms. The length of the final equation was fixed to seven descriptors. The linear option was used in the equation creation. Cross-validation was performed with the leave-one-out procedure. The PLS analysis was scaled, with all variables normalized to a variance of 1.0.

Use of alternate probes for calculating electrostatic descriptors. MFA was carried out initially with the generic probe, (H^+) representing the electrostatic interactions. However, the interaction energies between (H^+) and all the phosphate containing molecules were too high above the cutoff value, overemphasizing the electrostatic energy component. The activities of these molecules were therefore predicted incorrectly. To eliminate this artifact, NH_2 and H_2O were used as alternate probes, as outlined in the methods section above, to appropriately sample the electrostatic environment. The choice of these probes was appropriate because of the presence of seven positively charged residues (Arg14, Arg74, Arg95, Arg153, Arg156, Arg160, and Lys13) as well as a number of bound water molecules (Wat1002, Wat1003, Wat1009, Wat1012, Wat1014, Wat1018, Wat1022, Wat1024, Wat1026, and Wat1050) in the active site of $TMPK_{mt}$.

Table 1. Actual and predicted activities of training and test set molecules obtained from the three alignment methods

Compound	R^1	R^2	R^3	R^4	Actual activity, pK_i	Predicted activity, pK_i		
						Model I	Model II	Model III
1	CH_3	H	OH	$NHCOCH_3$	4.045	2.937[b]	4.045[a]	4.070[a]
2	CH_3	H	OH	N_3	5.154	4.815[a]	4.806[a]	5.165[a]
3	CH_3	H	OH	NH_2	4.920	4.505[b]	4.846[a]	4.774[a]
4	CH_3	OH	OH	OH	3.145	3.271[b]	4.619[b]	3.376[a]
5	CH_3	OH^c	OH	OH	3.623	3.755[a]	4.777[a]	3.350[a]
6	CF_3	H	OH	OH	4.013	3.718[a]	4.148[b]	3.737[b]
7	C_2H_5	H	OH	OH	2.940	3.009[a]	2.751[a]	3.090[a]
8	F	OH	OH	OH	3.283	2.903[a]	3.201[a]	3.520[a]
9	F	OH	OH	H	3.251	3.245[b]	3.275[a]	2.902[a]
10	CH_3	H	NH_2	OH	3.638	3.108[b]	3.318[a]	3.243[b]
11	CH_3	H	F	OH	4.552	4.531[a]	4.029[b]	4.314[a]
12	CH_3	F	OH	OH	3.913	4.263[b]	3.846[a]	3.683[a]
13	CH_3	OH	N_3	I	3.309	4.178[b]	4.103[b]	3.370[a]
14	CH_3	OH	NH_2	H	2.721	2.800[a]	2.934[a]	3.205[a]
15	CH_3	OH	$NHC(NH)NH_2$	OH	3.853	3.714[a]	4.221[b]	5.235[b]
16	CH_3	H	CH_2N_3	OPO_3^{2-}	4.920	4.694[a]	4.365[b]	5.019[a]
17	CH_3	H	CH_2NH_2	OPO_3^{2-}	4.978	4.824[a]	4.865[a]	4.581[b]
18	CH_3	H	CH_2F	OPO_3^{2-}	4.823	4.576[a]	4.978[a]	4.565[a]
19	CH_3	H	CH_2OH	OPO_3^{2-}	4.537	4.750[a]	4.395[a]	4.472[a]
20	CH_3	OH	CH_2N_3	OPO_3^{2-}	3.933	3.885[a]	4.047[a]	3.629[a]
21	CH_3	OH	CH_2NH_2	OPO_3^{2-}	3.501	3.775[b]	5.041[b]	3.938[b]
22	CH_3	H	CH_2N_3	OH	4.397	4.031[a]	4.049[b]	4.480[a]
23	CH_3	H	CH_2NH_2	OH	4.244	3.565[a]	3.344[b]	4.231[a]
24	CH_3	H	CH_2F	OH	4.346	4.374[a]	4.031[a]	3.559[b]
25	CH_3	H	CH_2OH	OH	4.387	3.851[b]	4.197[a]	4.527[a]
26	CH_3	OH	CH_2N_3	OH	3.113	3.499[a]	3.439[a]	3.864[b]
27	CH_3	OH	CH_2NH_2	OH	3.405	3.185[a]	3.372[a]	3.460[a]
28	CH_3	H	CH_2CH_2OH	OH	3.806	4.002[a]	4.089[a]	3.834[a]
29	CH_3	H	NH_2	OPO_3^{2-}	3.628	3.674[a]	4.005[a]	3.961[b]
30	CH_3	OH	NH_2	OPO_3^{2-}	4.568	4.415[b]	3.922[b]	4.502[a]
31	CH_3	NH_2	OH	OPO_3^{2-}	4.259	4.386[a]	4.804[a]	4.331[a]
32	CH_3	Cl	OH	OPO_3^{2-}	4.721	4.739[a]	4.560[a]	4.550[a]
33	CH_3	F	OH	OPO_3^{2-}	4.366	4.685[a]	4.535[a]	4.491[a]
34	$C_6H_5CH_2$	H	OH	OPO_3^{2-}	4.552	4.939[a]	4.414[a]	4.674[a]
35	CH_3	H	N_3	OPO_3^{2-}	5.000	4.827[a]	4.747[a]	5.707[b]
36	CH_3	H	N_3	OH	4.552	4.400[a]	4.585[a]	4.679[b]
37	Br	H	N_3	OH	4.978	4.820[a]	4.931[a]	5.136[a]
38	Br	H	OH	OH	5.301	5.074[a]	5.136[a]	5.193[a]
39	$CH=CHBr$	H	OH	OH	3.204	3.152[a]	3.423[a]	3.369[b]
40	CH_2OH	H	OH	OH	3.086	3.223[a]	3.203[a]	3.261[a]
41	Cl	H	N_3	OH	4.795	5.724[b]	4.511[a]	4.626[a]
42	CH_3	H	OH	OH	4.568	4.569[a]	4.816[a]	4.325[b]
43	H	H	OH	OH	2.991	4.022[b]	2.935[a]	3.477[a]
44	F	H	OH	OH	3.673	4.077[a]	4.009[b]	3.260[a]
45	I	H	OH	OH	4.481	4.885[a]	4.717[a]	4.744[a]
46	OH	H	OH	OH	3.568	3.619[a]	3.401[a]	3.353[a]
47	H	H	N_3	OH	3.091	3.148[a]	3.023[a]	2.434[b]

[a] Training set.
[b] Test set.
[c] Hydroxyl in β-position.

Three MFA models using different alignments namely least squares, pharmacophore, and receptor based methods were developed. The statistical details of all the three MFA models generated are summarized in

Table 2. The cross-validated r^2 (r_{cv}^2) of models I, II, and III are 0.790, 0.836, and 0.825, respectively. The predictive power of the three models is calculated by
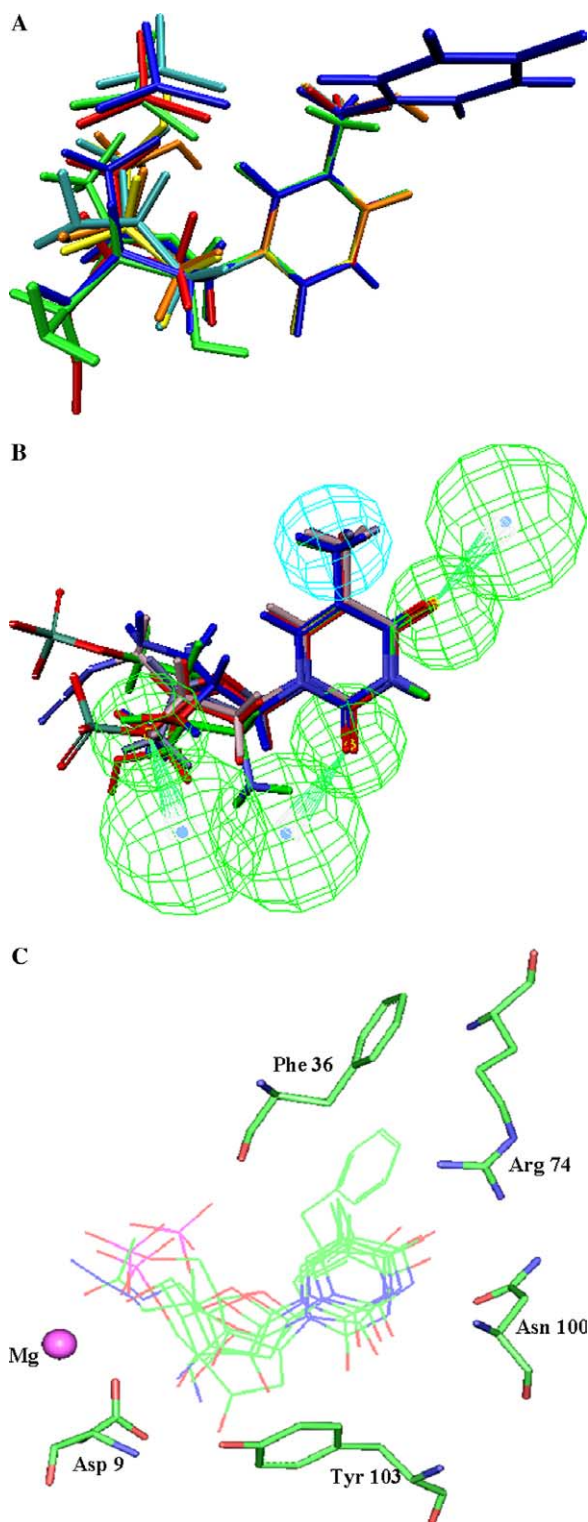
Figure 1. Alignment of study molecules using (A) least squares; (B) pharmacophore; and (C) docked conformations (only few representative molecules are shown for clarity).

$$r^2_{pred} = \frac{SD - PRESS}{SD},$$

where SD is the sum of squared deviations between the biological activities of each molecule and the mean activity of the training set molecules and PRESS is the sum of

Table 2. Statistical details of the MFA models obtained from three different alignment methods

	Least square (model I)	Pharmacophore (model II)	Docked conformations (model III)
r^2_{cv} [a]	0.790	0.836	0.825
r^2 [b]	0.905	0.915	0.907
PRESS [c]	3.800	3.147	2.990
r^2_{bs} [d]	0.874	0.910	0.903
r^2_{pred} [e]	0.705	0.560	0.722

[a] Cross-validated r^2.
[b] Conventional r^2.
[c] Predicted sum of squared residuals.
[d] Bootstrap r^2.
[e] Predictive r^2.

squared deviations between the predicted and the actual activities of molecules in the test set. Though the r^2_{cv} is better for the models II and III than model I, the predictive capability (r^2_{pred}) of model II (0.560) is less when compared to model III (0.722) and model I (0.705). The actual and predicted pK_i values of the training and the test set molecules for all the three models are given in Table 1. Scatter plots of actual against predicted activities for both the training and the test set molecules for the three different MFA models are given in Figure 2. Model III (receptor based) has marginally better statistics than other models. To assess the reliability of the docked conformations, initially the substrate of TMPK, dTMP, was docked into active site. The rmsd between the docked pose of dTMP and its bound conformation in the crystal structure (1G3U) is 0.2 Å, indicating that the docking method was able to reproduce the correct pose. Since receptor based alignment considers all the interactions made by each molecule with the active site residues, it determines the exact orientation of the molecule within the receptor. Thus, these conformations are much closer to the bioactive conformation of the molecules. Accordingly, the r^2_{cv} and r^2_{pred} values of model III are high.

The QSAR Eqs. 1–3 for all the three MFA models are described below. The steric (CH_3) and electrostatic (NH_2 and H_2O) descriptors in the equations specify the regions where structural variations in the ligands result in variation in the biological activity (Fig. 3). The numbers associated with the descriptor specify its location in the 3D-grid around the molecule. Model I (least squares alignment):

$$\begin{aligned}
Activity = {} & 3.31949 - 0.040242(CH_3/187) \\
& + 0.036577(H_2O/171) \\
& - 0.026125(H_2O/99) \\
& - 0.045066(H_2O/246) \\
& + 0.027542(CH_3/246) \\
& - 0.047336(H_2O/117) \\
& + 0.083325(CH_3/124).
\end{aligned} \quad (1)$$

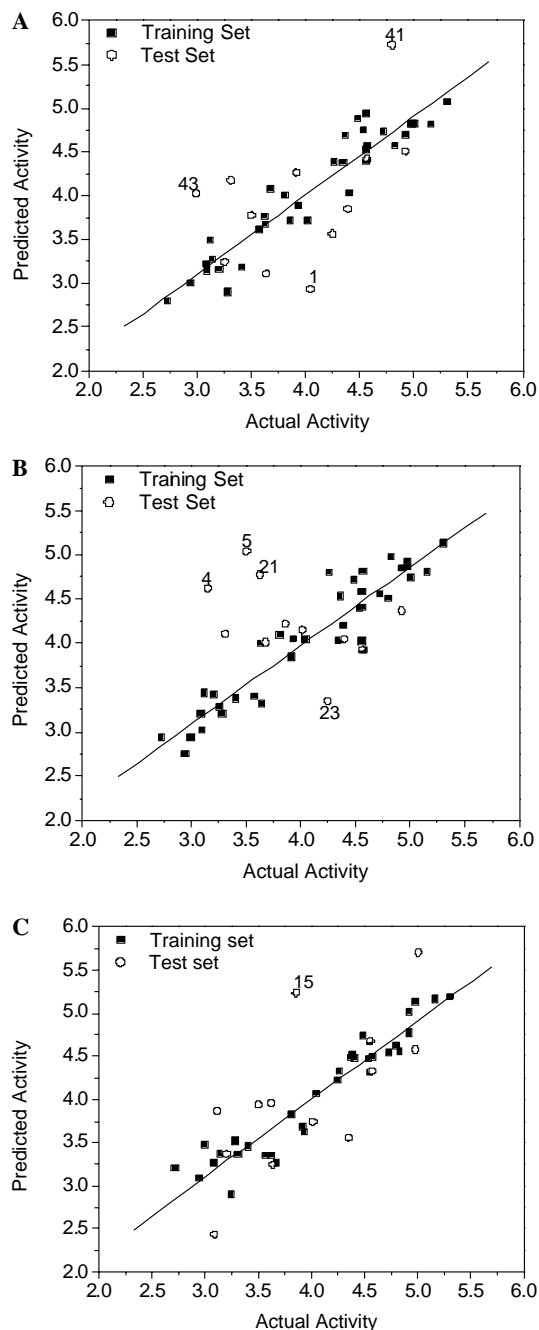Model II (pharmacophore based alignment):

Figure 2. Scatter plots of actual versus predicted activities of training and test molecules in (A) model I; (B) model II; and (C) model III. Molecules with higher residual values (outliers) are labeled.

$$
\begin{aligned}
\text{Activity} = \ &4.19631 + 0.03868(\text{H}_2\text{O}/218) \\
&- 0.026315(\text{CH}_3/685) \\
&- 0.031807(\text{NH}_2/398) \\
&+ 0.023836(\text{CH}_3/675) \\
&- 0.016316(\text{H}_2\text{O}/476) \\
&- 0.027176(\text{NH}_2/298) \\
&- 0.023874(\text{H}_2\text{O}/605).
\end{aligned}
\tag{2}
$$

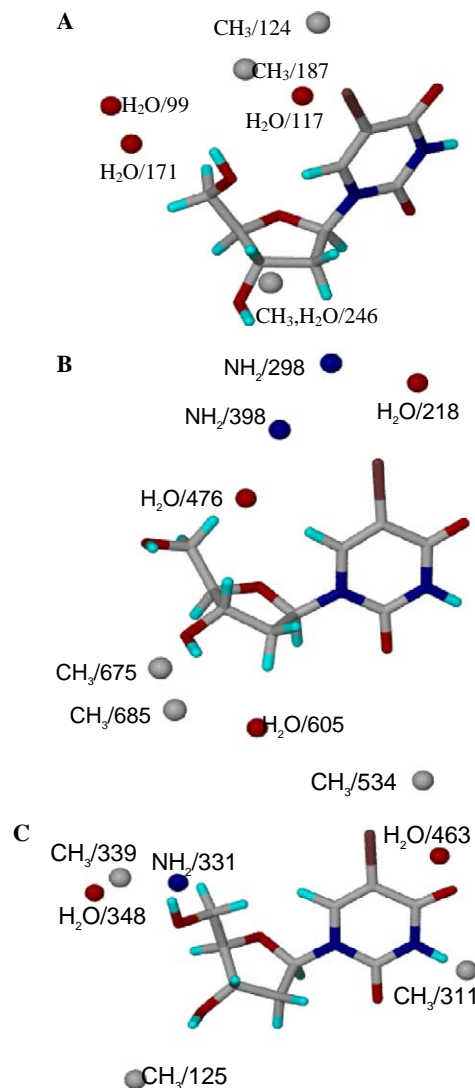Model III (receptor based alignment):

Figure 3. Mapping of 3D-descriptor points in the QSAR equations with most active molecule: (A) model I (least squares); (B) model II (pharmacophore); and (C) model III (docked conformations).

$$
\begin{aligned}
\text{Activity} = \ &2.37154 - 0.070375(\text{H}_2\text{O}/463) \\
&+ 0.054086(\text{CH}_3/534) \\
&+ 0.036304(\text{H}_2\text{O}/348) \\
&+ 0.043564(\text{CH}_3/311) \\
&+ 0.029729(\text{CH}_3/339) \\
&+ 0.045245(\text{CH}_3/125) \\
&- 0.011428(\text{NH}_2/331).
\end{aligned}
\tag{3}
$$

The results of all the three MFA models were compared and correlated with the predictive ability of the models. The appearance of steric descriptors ($\text{CH}_3/124$) and ($\text{CH}_3/187$) in model I and ($\text{CH}_3/534$) in model III at thymine C^5, indicates that moderately bulky substituents are favored at this position. However, in model II electronic descriptors like ($\text{NH}_2/298$) and ($\text{NH}_2/398$) occupy this position, indicating that electronegative groups are favored. Br fulfills these criteria and therefore molecule

38 shows the highest activity. The Br $\cdots$ O interaction at Phe36, and the extension of the cooperative network in the active site[14] concurs with the positioning of these descriptors. In model II the presence of (H_2O/605) near ribose $C^{2'}$ with a negative coefficient indicates that a hydrogen bond donor at this position may lead to decrease in activity. Hence, the higher activity of **22** and **23** with respect to **26** and **27** (which have a C^2 hydroxyl) is rationalized. This position is not well defined by the model I. The presence of steric descriptors (CH_3/246) in model I, (CH_3/675) in model II and (CH_3/125) in model III at ribose $C^{3'}$ indicates that bulky substituents are favored. Thus, molecules **16**, **17**, and **36** have higher activities than **19**, **29**, and **10**, respectively (Table 1). However, model II shows another steric descriptor (CH_3/685) with a negative coefficient at the same position indicating that bulkier substituents are not preferred. The extent of steric tolerance at this position is not well defined in models III and I. However, the coefficient of the descriptor at this position in model I is comparable with that in model II. Thus, molecule **15** with a bulky guanidine group is overestimated only in model III. The presence of (H_2O/246) at ribose $C^{3'}$ in model I also indicates that hydrogen bonding substituents are favored. The appearance of these descriptors is in good agreement with the that of the hydrogen bonds formed by the hydroxyl of dTMP with Asp9 and Wat1009 in the active site (Scheme 1). The presence of (H_2O/171) and (H_2O/99) in model I, (H_2O/476) in model II, and (H_2O/348) in model III near ribose $C^{5'}$ indicates that either hydrogen bond acceptors or donors can be accommodated favorably at this position. These represent the water molecules viz., Wat1050, Wat1018 occupying the co-ordination sites of the Mg^{2+} ion in the active site.[5] Further, the appearance of steric descriptors (CH_3/339) and electronic descriptor (NH_2/

331) in model III indicates that bulky and highly polar substituents are favored at this position. This is evident by the higher activities of **16**, **17**, **18**, **33**. and **35** containing phosphate groups at $C^{5'}$ vis-à-vis molecules **22**, **23**, **24**, **12**, and **36** that contain a hydroxyl at this position. Model I does not give any account of the steric requirements at this position. The outliers in each model were rationalized with reference to the location of the molecular descriptors. Based on the inability of model I to define the nature of substituents at $C^{2'}$ and $C^{5'}$, the least squares method was considered inferior to the other two alignment methods.

In the docking procedure, the conformation of each molecule is dictated by its interactions with the active site residues. However, in case of pharmacophore based alignment, less active molecules are not mapped properly to the pharmacophoric features. Therefore, the conformations of the less active molecules obtained from the pharmacophore based alignment may not be reasonable.[16] In the case of least squares method, it is assumed that all the molecules with a similar scaffold bind to the protein in a similar orientation. However, the substituents on the molecule may force a change in the orientation within the active site. Thus, neither of the alignment methods would give the molecular orientation accurately. This is reflected by the low r^2_{pred} value of models I and II. Therefore, receptor based alignment turns out to be superior to the other alignment methods.

All the 3D descriptors obtained in the model III concur with the active site residues of $TMPK_{mt}$. The steric descriptor CH_3/534 at thymine C^5 corresponds to the cavity formed by the residues Arg74, Phe36, Pro37, and Arg95. This cavity defines the volume of the substi-
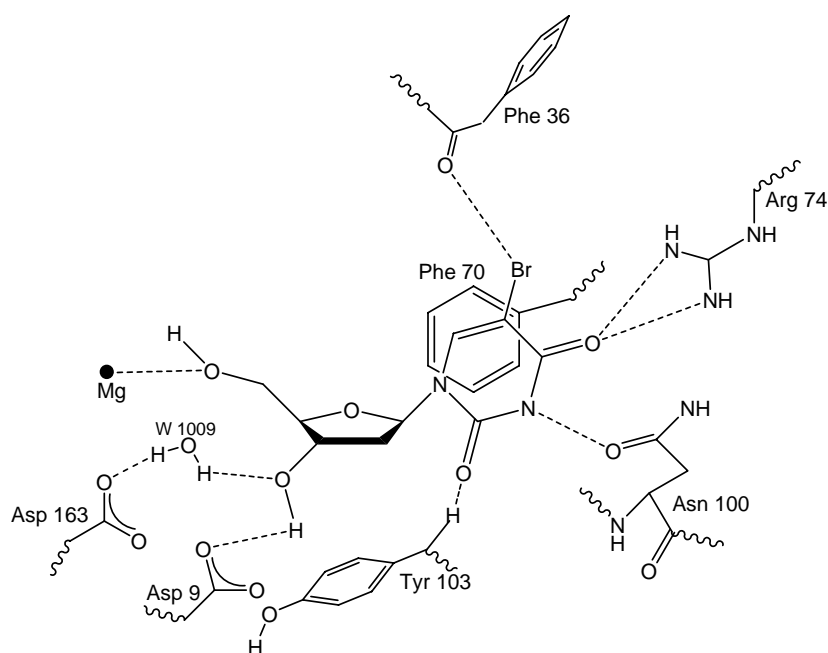
Scheme 1. Schematic representation of the most active molecule **38**-$TMPK_{mt}$ complex and the interactions within. Hydrogen bonds are shown as dashed lines.

tuent at this position. Also, the orientation of the backbone carbonyl of Phe36 makes it available for an electrostatic interaction with the substituent at this position (Scheme 1). Additionally, an electronic descriptor $H_2O/463$ at this position corresponds to a water molecule (Wat1012) in the active site. At $C^{3'}$ the appearance of steric descriptor $CH_3/125$ corresponds to the cavity lined by Asp9 and Asp163 indicating a bulkier positively charged substitution favorable at this position. AZTMP with an azido substitution at this position, therefore, shows a higher inhibitory activity.[10] Presence of steric and electronic descriptors like $CH_3/339$, $NH_2/331$, and $H_2O/348$ at $C^{5'}$ represents a bulky electronegative substituent required to interact with the Mg^{2+} ion present at this position and fill the cavity therein. Also, bulkier substituents at this position may displace the water molecules that occupy the co-ordination sites of the metal atom and thereby increase the inhibitory activity. Additionally, the scope of substitutions occupying the water positions and releasing the otherwise interlocked water molecules into the bulk would be entropically favorable.[17]

In conclusion, MFA models for $TMPK_{mt}$ inhibitors were developed using three different alignment techniques viz., least squares, pharmacophore based, and receptor based methods. The disposition of the 3D-descriptors obtained from the three models was similar. However, the receptor based MFA model shows predictivity higher than those of the other two models. In addition to the statistical quality, the 3D-descriptors obtained from receptor based model map well with the active site residues involved in the ligand binding. Br at C^5 position is not merely a cavity filler, but fulfills the electronic requirements as well. Bulkier substituents at $C^{3'}$ that can interact with the acidic residues increase the inhibitory activity. Bulkier electron-donating substitutions at $C^{5'}$ that can displace the water molecules from the co-ordination sites of Mg^{2+} ion may be entropically favorable for the ligand binding. The results provide useful information about the chemical and structural features of $TMPK_{mt}$ inhibitors and in designing new and potential antitubercular agents.

References and notes

1. Stokstad, E. *Science* **2000**, *287*, 2391.
2. WHO web pages on TB www.who.int/entity/tb/en.
3. Dye, C.; Williams, B. G.; Espinal, M. A.; Raviglione, M. C. *Science* **2002**, *295*, 2042.
4. Anderson, E. P.. In *The Enzymes*; Boyer, P. D., Ed.; Academic: New York, 1973; Vol. 8, p 49.
5. Sierra, L. D. L.; Munier Lehmann, H.; Gilles, A. M.; Bârzu, O.; Delarue, M. *J. Mol. Biol.* **2001**, *311*, 87.
6. Pochet, S.; Dugué, L.; Labesse, G.; Delepierre, M.; Munier-Lehmann, H. *ChemBioChem* **2003**, *4*, 742.
7. Vanheusden, V.; Munier-Lehmann, H.; Froeyen, M.; Dugué, L.; Heyerick, A.; Keukeleire, D. D.; Pochet, S.; Busson, R.; Herdewijn, P.; Calenbergh, S. V. *J. Med. Chem.* **2003**, *46*, 3811.
8. Vanheusden, V.; Munier-Lehmann, H.; Pochet, S.; Herdewijn, P.; Calenbergh, S. V. *Bioorg. Med. Chem. Lett.* **2002**, *12*, 2695.
9. Vanheusden, V.; Rompaey, P. V.; Munier-Lehmann, H.; Pochet, S.; Herdewijn, P.; Calenbergh, S. V. *Bioorg. Med. Chem. Lett.* **2003**, *13*, 3045.
10. Munier-Lehman, H.; Chaffotte, A.; Pochet, S.; Labesse, G. *Protein Sci.* **2001**, *10*, 1195.
11. Cho, S. J.; Tropsha, A. *J. Med. Chem.* **1995**, *38*, 1060.
12. Cerius² Molecular Modeling Program Package, Accelrys: San Diego, CA 92121-3752, USA.;
13. CATALYST Version 4.6; Accelrys: Burlington, MA.;
14. Gopalakrishnan, B.; Aparna, V.; Jeevan, J.; Ravi, M.; Desiraju, G. R. *J. Chem. Inf. Model.* **2005**, *45*, 1101.
15. GOLD 2.0, Cambridge Crystallographic Data Centre, 12 Union Road, Cambridge CB2 1EZ, UK.;
16. Zhu, L. L.; Hou, T. J.; Chen, L. R.; Xu, X. J. *J. Chem. Inf. Comput. Sci.* **2001**, *41*, 1032.
17. Ladbury, J. E. *Chem. Biol.* **1996**, *3*, 973.